

Article

Effective Removal of Ammonium from Aqueous Solution by Ball-Milled Biochar Modified with NaOH

Hefeng Yang ^{1,2}, Xiangming Li ¹, Yuting Wang ¹, Junxia Wang ¹, Lihong Yang ^{2,3}, Zhiqiang Ma ², Jipeng Luo ^{4,*}, Xiaoqiang Cui ^{1,*}, Beibei Yan ¹ and Guanyi Chen ^{1,5}

¹ Tianjin Key Lab of Biomass Waste Utilization, School of Environmental Science and Engineering, Tianjin University, Tianjin 300072, China

² CECEP DADI Environmental Remediation Co., Ltd., Beijing 100082, China

³ School of Environmental Science and Engineering, Southern University of Science and Technology, Shenzhen 518055, China

⁴ Key Laboratory of Environmental Remediation and Ecological Health, Ministry of Education, College of Environmental and Resource Sciences, Zhejiang University, Hangzhou 310058, China

⁵ School of Mechanical Engineering, Tianjin University of Commerce, Tianjin 300134, China

* Correspondence: luojp@zju.edu.cn (J.L.); cuixiaoqiang@tju.edu.cn (X.C.)

Abstract: The objective of this study was to investigate the feasibility of using modified biochars to enhance removal of ammonium from aqueous solution. The pristine, NaOH-modified, ball-milled, and NaOH-modified ball-milled biochars were prepared from wheat straw at 500 °C. The surface morphology and characteristics of biochar were obviously changed after modification. The NaOH-modification elevated the pH value and ash content of biochar, and the ball-milling treatment promoted the formation of oxygen-containing functional groups. The specific surface area of biochar ($20.9\text{ m}^2/\text{g}$) increased to $51.4\text{ m}^2/\text{g}$ and $145.6\text{ m}^2/\text{g}$ after NaOH-modification and ball-milling treatment, respectively. The modified biochars showed considerable ammonium sorption capacity in a wide pH range (3–7), and the optimal pH of ammonium sorption was around 6. Both NaOH-modification and ball-milling treatment improved ammonium sorption on the biochars. Ammonium sorption of the biochars could be well fitted by the Langmuir and pseudo-second-order model, and the NaOH-modified ball-milled biochar showed the highest ammonium sorption capacity of 8.93 mg g^{-1} . The surface complexation with oxygen-containing functional groups and cation exchange were the dominant mechanisms of ammonium sorption on the biochars. These results indicate that NaOH-modified/ball-milled biochar has a good potential to be used for the ammonium removal from polluted water.

Keywords: ammonium; biochar; sorption; modification; ball milling



Citation: Yang, H.; Li, X.; Wang, Y.; Wang, J.; Yang, L.; Ma, Z.; Luo, J.; Cui, X.; Yan, B.; Chen, G. Effective Removal of Ammonium from Aqueous Solution by Ball-Milled Biochar Modified with NaOH. *Processes* **2023**, *11*, 1671. <https://doi.org/10.3390/pr11061671>

Academic Editors: Carmen Branca and Gianni Andreottola

Received: 4 April 2023

Revised: 14 May 2023

Accepted: 23 May 2023

Published: 31 May 2023



Copyright: © 2023 by the authors. Licensee MDPI, Basel, Switzerland. This article is an open access article distributed under the terms and conditions of the Creative Commons Attribution (CC BY) license (<https://creativecommons.org/licenses/by/4.0/>).

1. Introduction

Nitrogen (N) is an essential element for plant growth and human health. In order to achieve a higher crop yield in response to the increasing population, more N-fertilizers have been produced and applied in the soils. However, the chemical N-fertilizer used in soils could release ammonium to water via runoff and leaching, resulting in serious eutrophication of surface water [1–3]. According to the environmental status bulletin of China in 2020, eutrophic surface water (i.e., reservoirs and lakes) accounted for 29.0% of the total water bodies [4]. Hence, several techniques have been developed to remove ammonium from water, such as sorption, ion exchange, biofilm reactors, membrane separation, and phytoremediation [5–9]. Among these removal approaches, sorption has been extensively employed due to its cost-effectiveness and environmental friendliness. For the sorption scheme, the sorbent was crucial to the pollutant removal efficiency, and thus the green sorbent with low cost and high efficiency is urgently needed for ammonium removal.

Biochar is a carbonaceous solid material derived from the pyrolysis of biomass under oxygen-limited conditions [10]. Biochar has shown great potential in the fields of soil improvement, carbon sequestration, and environmental remediation [11–14]. Recently, it was applied to remove ammonium from aqueous solution as a potential sorbent, and the ammonium sorption capacity of biochar was determined by the feedstock properties and production parameters (e.g., pyrolysis temperature, heating rate, and residence time) [15–17]. Cui et al. compared the ammonium sorption capacity of biochars derived from different species of aquatic plants at 500 °C and found that the *Canna indica*-derived biochar had the highest ammonium sorption capacity due to higher content of oxygen-containing functional groups [5]. Ion exchange is also an important mechanism for ammonium adsorption. Gai et al. indicated that the biochar with the highest cation exchange capacity showed the highest ammonium removal efficiency [18]. Tang et al. investigated the effect of pyrolysis temperature (350–550 °C) on the ammonium sorption capacity of biochar and indicated that biochar produced at 450 °C showed the greatest ammonium sorption capacity (1.4 mg/g) owing to its higher functional group density and specific surface area [16]. Notably, the biochars after ammonium sorption could be reused as additive or organic fertilizer for soil improvement [19], providing a potentially cyclic utilization scheme of nutrient. Nevertheless, considering the limited ammonium sorption capacity of raw biomass-derived biochar, it is necessary to modify the biochars to effectively remove more ammonium from water.

In order to improve the ammonium sorption capacity of biochar, several modification strategies have been investigated, including metal oxides/metal doping, alkaline treatment, and granulation [15,20–22]. Vu et al. reported that the corncob derived biochar showed a highest adsorption capacity of 22.6 mg NH₄⁺-N/g after modification with HNO₃ and NaOH [22]. Wang et al. found that the FeCl₃-HCl modification improved the ammonium sorption capacity of biochar by 14% owing to the increased specific surface area and functional groups (–OH and O–C=O) [23]. Moreover, ball milling has emerged as an effective approach for the syntheses and modification of carbon/metal nanomaterials due to its merits of low cost, high efficiency, and environmental friendliness [24,25]. Recently, ball-milling is considered a promising modification method to enhance the physicochemical properties of biochar via improving the specific surface area and creating new functional groups/defects on the surface [25–27], which are expected to improve the ammonium sorption capacity of biochars. However, quite limited study determined the potential of ball-milled biochar in ammonium removal from water [28]. Moreover, no study investigates the feasibility of combining ball-milling with other modification methods to enhance the ammonium sorption capacity of biochar, and the corresponding ammonium sorption mechanisms of dually modified biochar should be clarified.

In the present study, the dually modified biochars were synthesized and evaluated for their ammonium sorption capacity. The pristine biochar was prepared from wheat straw by pyrolysis at 500 °C, and the modified biochars were treated with alkali (NaOH) and ball-milling. After systematical characterization of the raw and modified biochars, sorption kinetics and isotherm of ammonium on biochars were conducted. The objectives of this study were to (1) develop a feasible modification strategy of biochar for ammonium removal, (2) characterize the physicochemical properties of the modified biochars, and (3) determine the sorption capacity and mechanisms of the modified biochars.

2. Materials and Methods

2.1. Preparation of the Pristine and Modified Biochars

The dried wheat straw samples were ground into ~1 mm powder using a stainless grinding machine for the biochar production. The production of wheat straw biochar was carried out in a modified muffle furnace (Sante Furnace 30–3000 °C, SAF-Therm, Henan, China) under N₂ atmosphere, and the pyrolysis of biomass (10 g) was programmed to drive the temperature to 500 °C at a rate of 5 °C/min and held for 2 h. The solid residues from pyrolysis were ground in a mortar and sieved through a 20-mesh sieve prior to use,

and the product was named as wheat straw biochar (WB). For the preparation of alkali modified biochar, the wheat straw was added into 1 mol/L NaOH at a ratio of 1 g:1 mL, and the mixed solution was held for 12 h after mixing well. The alkali modified wheat straw biochar (AWB) was obtained by pyrolyzing the abovementioned alkali modified wheat straw under the same pyrolysis conditions. In order to prepare ball-milled biochars, WB and AWB were placed in the agate jars of a planetary ball mill (DECO-PBM-1L-A, Jiangsu, China). Ball milling was operated at 500 rpm with a mass ratio of 1:20 (biochar to ball) for 8 h, and the direction of rotation changed every 10 min. The derived ball-milled biochars were referred to as ball-milled wheat straw biochar (B-WB) and ball-milled alkali-modified wheat straw biochar (B-AWB), respectively.

2.2. Characterization

Elemental contents (carbon, hydrogen, and nitrogen) of biochar samples were analyzed using a UNICUBE analyzer (Elementar). Fourier transform infrared (FTIR) analysis was employed to determine the functional group composition of biochar in the wavenumber range of 500–4000 cm⁻¹ in the form of KBr tablet using an FTIR spectrophotometer (IRAffinity-1S). In order to identify the crystalline structures of biochar, X-ray diffraction analysis (XRD, X' Pert Pro MPD) was carried out at 40 mA and 40 kV using Cu Ka radiation, and the scanning angle was 5–90°. The ash content was measured by placing biochar samples in a muffle furnace and heating to 750 °C for 5 h. The pH of biochar was measured using a pH meter (PHSJ-3F, INESA, Shanghai, China) by adding samples to deionized water at a mass/water ratio of 1:20. The size distribution of biochar was determined using a Malvern Mastersizer.

2.3. Sorption Experiment

Ammonium stock solutions were prepared by dissolving ammonium chloride (NH₄Cl) in deionized water. In order to investigate the effect of pH on the ammonium sorption, the biochar (0.1 g) was added into 30 mL solutions containing 30 mg ammonium-N L⁻¹ with an initial pH range between 3.0 and 7.0, which was adjusted by using 0.5 M HCl or NaOH solutions. The final pH in the solutions and the ammonium sorption capacity of biochar were determined after shaken at 120 rpm and 25 °C for 24 h. Sorption kinetics of ammonium was determined in the solutions containing 30 mg ammonium-N L⁻¹ under the aforementioned conditions, and the samples were taken and analyzed at various time intervals (0, 5 min, 15 min, 30 min, 1 h, 2 h, 4 h, 7 h, 12 h, and 24 h). Sorption isotherm of ammonium was investigated in the solutions containing different ammonium-N concentrations (0–200 mg/L) under the aforementioned conditions. The biochars after ammonium-N sorption are named as WB-N, AWB-N, B-WB-N, and B-AWB-N, respectively. The biochars after ammonium-N sorption were filtrated and dried at 80 °C for FTIR analysis. The concentrations of ammonium in the solutions were analyzed by colorimetric method. The amount of ammonium sorbed on biochar (Q_t) was calculated by the ammonium-N concentration difference between the initial and equilibrium solutions:

$$Q_t = (C_0 - C_t)V/m \quad (1)$$

where C_0 and C_t (mg/L) are the ammonium-N concentrations at initial and time t, respectively, V is the volume of the aqueous solution (L), and m is the dry weight of biochar (g) used in the sorption experiment. The contribution of cation exchange to the ammonium sorption was investigated in the solution containing 200 mg ammonium-N L⁻¹ and deionized water, which was described in our previous study [5].

2.4. Statistical Analysis

Statistical analysis was conducted by the SPSS 20.0, and the mean value and standard deviation were calculated via descriptive statistics. The data were tested at the significant level of $p < 0.05$ using one-way ANOVA. The correlation analysis was conducted with the Pearson test at $p < 0.05$ by SPSS 22.0.

3. Results and Discussion

3.1. Effects of Modification on Biochar Properties

The basic physicochemical characteristics of the raw and modified biochars derived from wheat straw are listed in Table 1. The NaOH-modified biochar (AWB) showed a higher pH (11.0) than the raw wheat straw biochar (WB, pH = 10.3), which resulted from the addition of NaOH during the pyrolysis process. Accordingly, the ash content of AWB (54.22%) was significantly higher than WB (50.19%) ($p < 0.01$). After ball-milling treatment, the pH value of B-WB and B-AWB decreased to 9.3 and 10.5, respectively. The reduction in the pH values of ball-milled biochars could be ascribed to the formation of acidic functional groups (e.g., $-\text{COOH}$) during the ball milling process. In comparison with WB and AWB, B-WB and B-AWB had higher H/C and O/C ratios, indicating that the ball milling favored the formation of less aromatic structures and hydrophilic surfaces of biochar, in agreement with the previous study [25]. The hydrophilic property of ball-milled biochar is expected to promote the sorption of the polar contaminants such as ammonium.

Table 1. The basic physicochemical properties of the raw and modified biochars.

Sample ^a	pH	Ash	N (%)	C	H	O	O/C	Atomic Ratio H/C	(O + N)/C	SSA (m ² /g)
WB	10.25 ± 0.02	50.19 ± 0.37	0.82	38.16	1.764	8.62	0.17	0.55	0.19	20.9
AWB	11.01 ± 0.00	54.22 ± 0.75	0.46	32.18	1.583	11.44	0.27	0.59	0.28	51.4
B-WB	9.25 ± 0.01	48.79 ± 0.20	0.81	37.74	1.978	10.38	0.21	0.63	0.22	145.6
B-AWB	10.53 ± 0.01	51.06 ± 0.26	0.53	33.11	1.884	13.34	0.30	0.68	0.32	121.7

^a: WB, wheat straw biochar; AWB, NaOH-modified wheat straw biochar; B-WB, ball-milled wheat straw biochar; B-AWB, ball-milled and NaOH-modified wheat straw biochar.

As presented in Table 1, the specific surface area of biochar ranged from 20.9 to 145.6 m²/g depending on the modification technique. The specific surface area elevated from 20.9 to 51.4 m²/g after NaOH-modification, and this value increased to 145.6 m²/g after ball-milling treatment. However, the specific surface area of B-AWB (121.7 m²/g) is lower than that of B-WB. The decreased specific surface area of B-AWB was probably due to the merging of micropore and a partial occlusion of the pores by the additive during the ball-milling process. This implies that both NaOH-modification and ball milling increased the specific surface area of biochar, which is consistent with the previous studies [1,25,29,30]. Notably, ball milling showed a much better potential to elevate the specific surface area of biochar due to the mechanism difference. The addition of NaOH could create new pores and widen the existing pores [29], while ball milling could increase the external surface area by reducing particle size and elevate the internal surface area via improving internal porosity [25]. The surface morphology of the pristine and modified biochars was presented in the SEM images (Figure 1). In comparison with the rough surface of the unmilled biochars (WB and AWB), the ball-milled biochars had more ultrafine particles, which was consistent with the size distribution results (Figure 2).

Figure 3a illustrates the FTIR spectra of raw and modified biochars. A wide spectrum of the functional group peaks, including $-\text{OH}$ at around 3400 cm⁻¹, aromatic C=C/C=O at 1603 cm⁻¹, CH₂ at 1376 and 1436 cm⁻¹, and C—O/C—O—C at 1090 cm⁻¹ were well preserved on the surface of the raw biochar. After modification with NaOH and ball-milling treatments, more functional group peaks were observed in the FTIR spectra of AWB, B-WB, and B-AWB. After ball milling of biochar, the corresponding vibration peaks at ~3400, 1603, and 1090 cm⁻¹ were significantly enhanced in the spectrum of B-WB (Figure 3a), indicating that ball milling could elevate the contents of oxygen-containing functional groups (e.g., $-\text{OH}$, C=O, and C—O) in the biochar, which is consistent with the element analysis results (Table 1) and the previous studies [1,27]. Similarly, more oxygen-containing functional groups were retained in B-AWB compared with AWB, and the enhancement of oxygen-containing functional groups could promote the sorption capacity of ammonium [5,23]. As depicted in Figure 3b, SiO₂ and KCl were the dominant mineral crystals in the XRD pattern of WB. After NaOH-modification and ball-milling treatments,

the intensity of SiO_2 diffraction peak increased in the modified biochars, implying that both NaOH modification and ball milling favored the development of SiO_2 crystal, in good agreement with the FTIR results (Figure 3b).

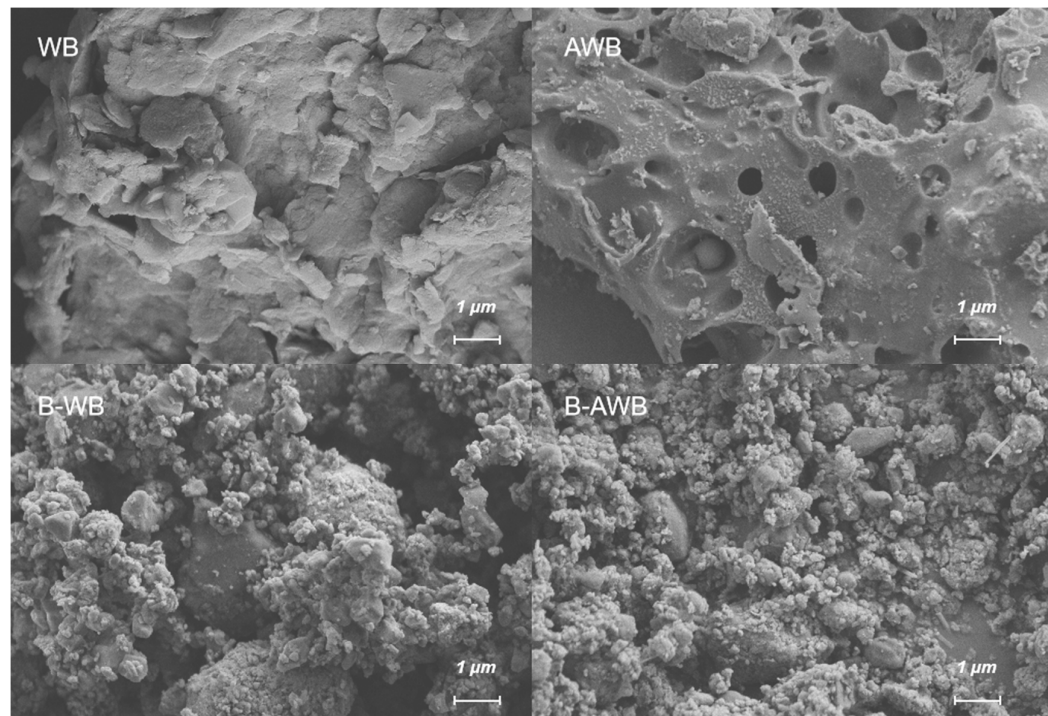


Figure 1. SEM images of the raw and modified biochars. WB, wheat straw biochar; AWB, NaOH-modified wheat straw biochar; B-WB, ball-milled wheat straw biochar; B-AWB, ball-milled and NaOH-modified wheat straw biochar.

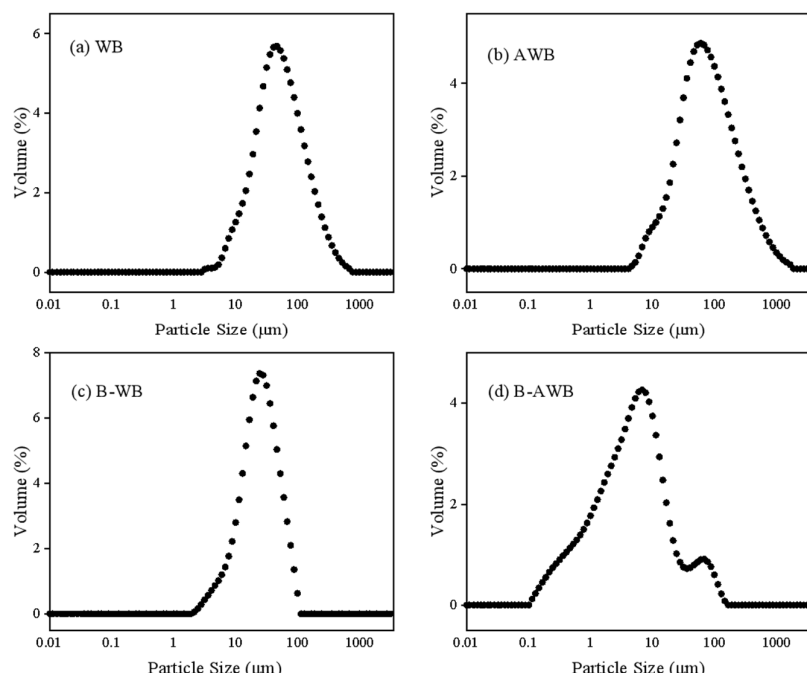


Figure 2. The size distribution of the raw and modified biochars. (a) WB, wheat straw biochar; (b) AWB, NaOH-modified wheat straw biochar; (c) B-WB, ball-milled wheat straw biochar; (d) B-AWB, ball-milled and NaOH-modified wheat straw biochar.

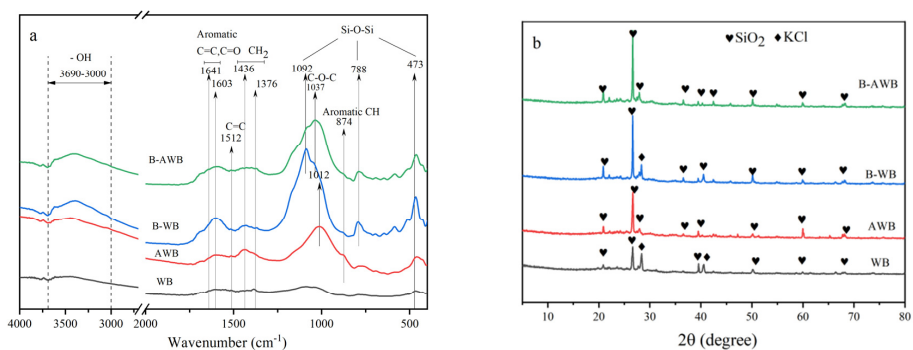


Figure 3. (a) The FTIR spectra of the raw and modified biochars; (b) XRD patterns of the raw and modified biochars.

3.2. Ammonium Sorption

3.2.1. pH Dependent Sorption

The effect of aqueous solution pH on ammonium sorption onto the raw and modified biochars is presented in Figure 4. The results demonstrate that the ammonium sorption capacity of biochars was pH dependent. Generally, the modified biochars showed considerable ammonium sorption capacity in a wide pH range, and the optimal pH of ammonium sorption was around 6 in this study. As depicted in Figure 4, the amount of adsorbed ammonium increased with increasing pH from 3 to 6 and slightly declined as pH elevated to 7. Similar trends were found in the previous studies [15,16]. The lower ammonium sorption capacity at lower pH could be attributed to the competition between NH₄⁺ and H⁺ for the interaction with the functional groups on the biochar surface. This competition was weakened with the decrease of H⁺ at higher pH, and more ammonium was adsorbed onto the biochars. Additionally, the more negatively charged surface of biochar at higher pH of aqueous solution favored the ammonium adsorption via electrostatic attraction [1,22]. The decrease of ammonium removal at pH > 6 could be ascribed to the fact that some of the ammonium is converted to NH₃·H₂O, which suppressed the sorption process [21]. In comparison with the raw biochar, the ammonium sorption capacity of the modified biochars was more sensitive to the pH change. This phenomenon could be attributed to the more abundant oxygen-containing functional groups on the modified biochars. The interaction between the oxygen-containing functional groups and ammonium was considered a main mechanism of ammonium sorption of biochar [5,15,23], and the chemical state of the oxygen-containing functional groups on the biochar surface was greatly affected by the pH of aqueous solution [31]. For instance, carboxyl groups are acidic groups generally having pKa < 5, and these groups could dissociate with increasing pH.

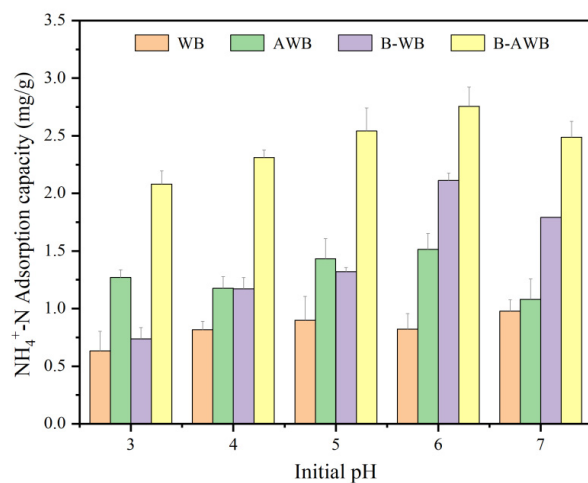


Figure 4. Effect of pH on ammonium sorption on the raw and modified biochars.

3.2.2. Ammonium Sorption Kinetics

Kinetics models were employed to study the reaction dynamics of ammonium sorption onto the raw and modified biochars. As presented in Figure 5, the ammonium sorption onto the raw biochar sharply elevated in the first 1 h, accounting for around 93.2% of the final sorption capacity, and reached saturation in 7 h. Similarly, the ammonium sorption equilibrium was reached within 4 h for the modified biochars. To further analyze the ammonium sorption process onto different biochars, the pseudo-first-order and the pseudo-second-order sorption kinetics models were employed to fit the experimental data. As shown in Table 2, the pseudo-first-order model ($R^2 = 0.95$) better fitted the ammonium sorption data for the raw biochar than that of the pseudo-second-order model ($R^2 = 0.92$), while for the NaOH-modified and ball-milled biochars, the fitting degree of the pseudo-second-order model ($0.95 \leq R^2 \leq 0.98$) was better than that of the pseudo-first-order model ($0.94 \leq R^2 \leq 0.98$). Additionally, the predicted ammonium-N sorption capacity of the modified biochars (1.12–2.12 mg/g) by the pseudo-second-order kinetics model was more close to the experimental values (1.14–2.17 mg/g). The fitting results implies that the ammonium sorption onto the modified biochars was mainly dominated by chemical interaction, which is in accordance with the previous studies [5,16], further confirming that more active sites (e.g., oxygen-containing functional groups) for ammonium sorption were successfully introduced after NaOH-modification and ball-milling treatments. Furthermore, the sorption rate constant K_1/K_2 fitted by the sorption kinetics of the modified biochars was larger than that of the raw biochars, in a good agreement with the experimental phenomenon, indicating good application potential of the modified biochars.

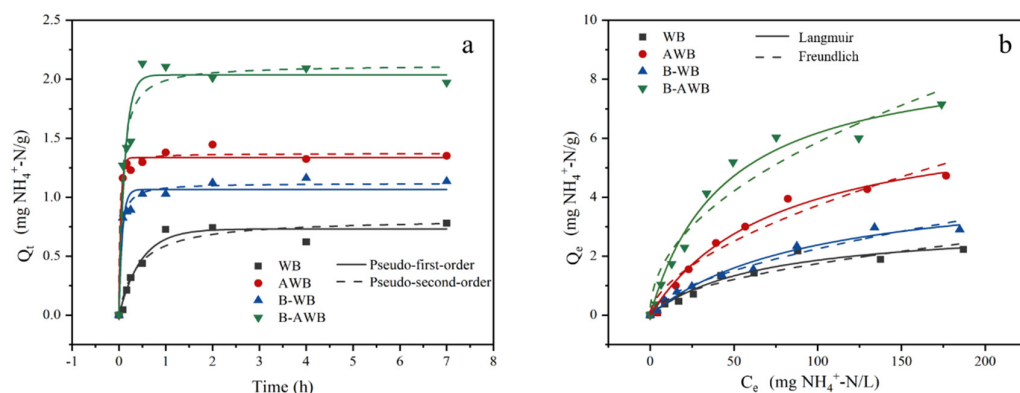


Figure 5. (a) Sorption kinetics and (b) isotherm of ammonium on the raw and modified biochars. The symbols and lines are the experimental and modeled results, respectively. (ammonium-N concentration, 0–200 mg/L; adsorbent dose, 3.3 g/L; adsorption time, 0–7 h; adsorption temperature, 25 °C).

Table 2. Sorption parameters of ammonium on the raw and modified biochars obtained from the different kinetics models.

Biochar	Pseudo-First-Order ^a			Pseudo-Second-Order ^b		
	$q_t = q_e (1 - e^{-k_1 t})$		R^2	$q_t = k_2 q_e^2 t / (1 + k_2 q_e t)$		R^2
	k_1 (h ⁻¹)	Q_e (mg/g)		k_2 (g/mg·h)	Q_e (mg/g)	
WB	2.13	0.73	0.95	3.11	0.82	0.92
AWB	23.57	1.34	0.98	46.56	1.37	0.98
B-WB	13.86	1.06	0.94	22.54	1.12	0.98
B-AWB	7.98	2.04	0.94	7.09	2.12	0.95

^a: Q_t is the amount of ammonium sorption at equilibrium, mg g⁻¹, K_1 is the rate constant of pseudo-first-order model (h⁻¹), Q_e is the sorption capacity at equilibrium calculated by the pseudo-first-order model, mg g⁻¹; ^b: Q_t is the amount of ammonium sorption at equilibrium, mg g⁻¹, K_2 is the rate constant of the pseudo-second-order reaction (g mg⁻¹ h⁻¹), Q_e is the sorption capacity at equilibrium calculated by the pseudo-second-order model, mg g⁻¹.

3.2.3. Ammonium Sorption Isotherm

The sorption isotherms of ammonium onto the raw and modified biochars are shown in Figure 5b, and the fitted parameters are summarized in Table 3. The amount of adsorbed ammonium-N by biochar was elevated with increasing initial ammonium concentration. In comparison with the raw biochar, the modified biochars exhibited higher sorption capacity for ammonium-N. The ammonium adsorption behaviors were described using the Langmuir and Freundlich adsorption isotherm models. The Langmuir equation fitted the ammonium sorption data of the raw and modified biochars better than the Freundlich equation, with correlation coefficients (R^2) in the range of 0.95–0.99. The better fitting of sorption data to the Langmuir model implies that the ammonium adsorption occurred largely in a monolayer on the homogeneous surface of biochar, which is consistent with the previous studies [5,16]. The maximum sorption of ammonium-N (Q_m) on B-AWB was 8.93 mg g^{-1} , approximately three times that of WB (3.09 mg g^{-1}). In comparison, B-WB (4.64 mg g^{-1}) and AWB (6.93 mg g^{-1}) had moderate maximum sorption capacity for ammonium-N according to the Langmuir model. These results indicate that both NaOH modification and ball milling improved the ammonium-N sorption capacity of biochar, and the dual modification exhibited enhancement to the ammonium sorption. The maximum ammonium-N sorption capacity of B-AWB is higher than that of biochars derived from rice husk (3.24 mg/g), pine sawdust ($3.37\text{--}5.38 \text{ mg/g}$), and giant reed ($1.21\text{--}1.49 \text{ mg/g}$) in the previous studies [32–34], indicating that the modified wheat straw biochar has a good potential for the treatment of ammonium-contaminated water. Furthermore, Table 4 summarizes the ammonium sorption capacity of different biochars in the previous studies.

Table 3. Sorption parameters of ammonium on the raw and modified biochars obtained from the different isotherm models.

Biochar	Langmuir ^a			Freundlich ^b		
	$q_e = K_L C_e q_m / (1 + K_L C_e)$			$K_F (\text{mg/g})$	N	R^2
	$K_L (\text{L/mg})$	$Q_m (\text{mg/g})$	R^2			
WB	0.02	3.09	0.95	0.15	0.53	0.89
AWB	0.01	6.93	0.99	0.26	0.57	0.95
B-WB	0.03	4.64	0.98	0.16	0.58	0.96
B-AWB	0.02	8.93	0.98	0.65	0.48	0.92

^a: Q_m is the maximum sorption capacity (mg g^{-1}), C_e is the concentration of ammonium after sorption, K_L is the affinity coefficient of Langmuir model; ^b: Q_m is the maximum sorption capacity (mg g^{-1}), C_e is the concentration of ammonium after sorption, K_F is the experimentally derived capacity coefficient of Freundlich model (mg g^{-1}), N is experimentally derived exponent of Freundlich model.

Table 4. Ammonium sorption capacity of different biochars in previous study.

Adsorbents	Modification Method	Solid-Liquid Ratio (g/L)	Sorption Capacity (mg/g)
Bamboo biochar [15]	Unmodified	1.00	4.96
Digested sludge [16]	Unmodified	10.00	1.40
Rice straw [20]	Unmodified	1.60	3.20
Rice straw [20]	Potassium-iron modified	1.60	10.77
Pine wood chips biochar [35]	Unmodified	1.00	2.86
Reed waste biochar [36]	Unmodified	5.00	1.92
Reed waste biochar [36]	Sulfonation modified	10.00	5.19
Orange peel [37]	Unmodified	10.00	4.36
B-AWB (this study)	NaOH-ball-milled modified	3.33	8.93

3.3. Ammonium Sorption Mechanisms on the Modified Biochars

The oxygen-containing functional groups were crucial to the ammonium sorption onto biochars [5,20,23,38]. As depicted in Figure 3a, more oxygen-containing functional groups (e.g., $-\text{OH}$, $\text{C}=\text{O}$, and $\text{C}-\text{O}$) were formed in the biochar after NaOH modification and ball milling, and the ammonium-N sorption capacity of the modified biochars was greatly enhanced (Figure 5b). Correspondingly, B-AWB with most abundant oxygen-containing functional groups exhibited the highest ammonium-N sorption capacity. Moreover, the amount of ammonium-N sorbed on biochars was significantly correlated with the O/C ratio of biochar ($r = 0.993$, $p < 0.01$), implying that oxygen-containing functional groups is involved in ammonium sorption onto biochars. As presented in Figure 6, obvious changes could be observed on the FTIR spectra of biochar at the peaks of $\text{C}-\text{O}-\text{C}$ and $\text{C}=\text{O}$ after ammonium-N sorption, which is consistent with the previous studies [5,23]. These results demonstrate that the oxygen-containing functional groups play a dominant role in the ammonium sorption onto biochar.

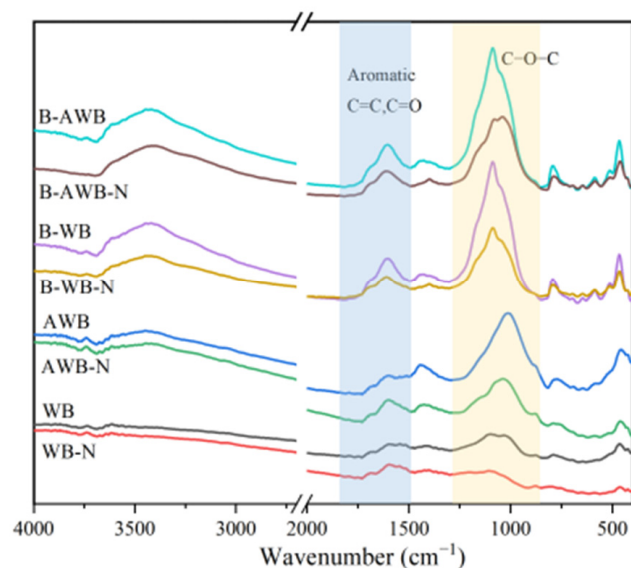


Figure 6. FTIR spectra of biochars before and after ammonium sorption.

In addition to the contribution of oxygen-containing functional groups, the role of cation exchange is also should be taken into consideration for ammonium sorption of biochars. A significant amount of metal ions (e.g., K^+ , Na^+ , Ca^{2+} , and Mg^{2+}) remained on the biochars via forming complexes with oxygen-containing functional groups, electrostatic attraction, and precipitation. Cui et al. reported that the ammonium-N sorption capacity of biochar was highly correlated with the amount of Mg^{2+} and Ca^{2+} released after ammonium sorption [5], and a similar trend was reported by Zheng et al. [39]. To investigate the role of cation exchange in ammonium sorption, the amount of metal ions released in solution before and after ammonium sorption on biochar was determined in this study. As illustrated in Figure 7, the obvious release of Ca^{2+} , K^+ , Mg^{2+} , and Na^+ occurred during the ammonium sorption process. This demonstrates that cation exchange occurred during the ammonium sorption onto the biochars. However, the total amounts of cations released from biochar after sorption were not highly correlated with the ammonium-N sorption capacity of biochar ($p > 0.05$), suggesting that the cation exchange was not the dominant ammonium sorption mechanism of biochars in the present study.

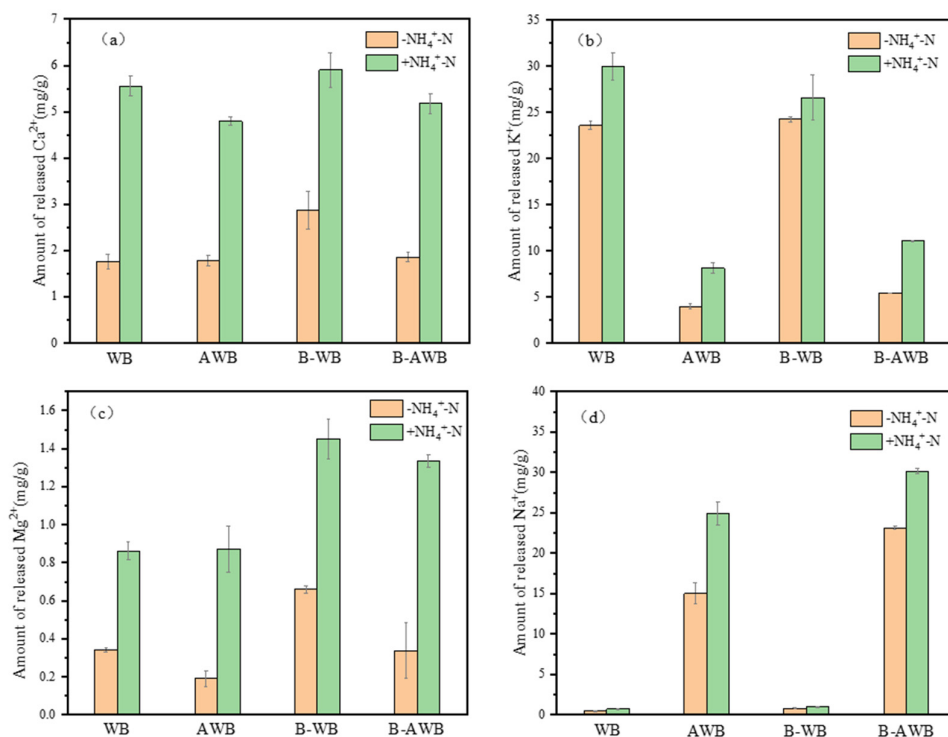


Figure 7. (a) The amount of Ca^{2+} released from biochars into solution before ($-\text{NH}_4^+ - \text{N}$) and after ($+\text{NH}_4^+ - \text{N}$) ammonium sorption; (b) the amount of K^+ released from biochars into solution before ($-\text{NH}_4^+ - \text{N}$) and after ($+\text{NH}_4^+ - \text{N}$) ammonium sorption; (c) the amount of Mg^{2+} released from biochars into solution before ($-\text{NH}_4^+ - \text{N}$) and after ($+\text{NH}_4^+ - \text{N}$) ammonium sorption; (d) the amount of Na^+ released from biochars into solution before ($-\text{NH}_4^+ - \text{N}$) and after ($+\text{NH}_4^+ - \text{N}$) ammonium sorption.

4. Conclusions

NaOH-modified/ball-milled biochars derived from wheat straw were prepared and employed for the effective ammonium removal from aqueous solutions, and the dual modification exhibited enhancement to the ammonium sorption. In comparison with the raw biochar, the physicochemical properties of the modified biochars were obviously changed. Considering the low cost of NaOH/ball-milling modifications and wheat straw feedstock, the NaOH-modified/ball-milled wheat straw biochar could be used as an effective adsorbent for ammonium removal. Furthermore, ammonium-N is an essential nutrient for plant growth, and thus the N-laden biochars after ammonium sorption have a good potential as an alternative fertilizer. However, the toxicity assessment and field trials should be conducted before the large-scale soil application of the N-laden biochars after ammonium sorption.

Author Contributions: H.Y.: Conceptualization, Writing—Original draft preparation, Funding acquisition. X.L.: Conceptualization, Methodology, Validation, Formal analysis, Writing—Original draft preparation. Y.W.: Resources, Investigation. J.W.: Software, Visualization. L.Y.: Resources, Data supply. Z.M.: Resources, Data supply. J.L.: Writing—review & editing, Supervision. X.C.: Conceptualization, Methodology, Resources, Writing—original draft & editing, Supervision. B.Y.: Project administration. G.C.: Writing—review & editing, Funding acquisition, Supervision. All authors have read and agreed to the published version of the manuscript.

Funding: This research was funded by Ministry of Science and Technology of the People's Republic of China (2021YFE0102500) and CECEP DADI Environmental Remediation Co., Ltd. (2021GKF-0474).

Data Availability Statement: Data will be made available on request.

Conflicts of Interest: There are no conflict of interest to declare.

References

- Qin, Y.; Zhu, X.; Su, Q.; Anumah, A.; Gao, B.; Lyu, W.; Zhou, X.; Xing, Y.; Wang, B. Enhanced removal of ammonium from water by ball-milled biochar. *Environ. Geochem. Health* **2020**, *42*, 1579–1587. [[CrossRef](#)] [[PubMed](#)]
- Conley, D.J.; Paerl, H.W.; Howarth, R.W.; Boesch, D.F.; Seitzinger, S.P.; Havens, K.E.; Lancelot, C.; Likens, G.E. Controlling Eutrophication: Nitrogen and Phosphorus. *Science* **2009**, *323*, 1014–1015. [[CrossRef](#)] [[PubMed](#)]
- Cameron, K.C.; Di, H.J.; Moir, J.L. Nitrogen losses from the soil/plant system: A review. *Ann. Appl. Biol.* **2013**, *162*, 145–173. [[CrossRef](#)]
- MEPC. *China Environmental Status Bulletin in 2020*; Ministry of Environment Protection of the People’s Republic of China: Beijing, China, 2021.
- Cui, X.; Hao, H.; Zhang, C.; He, Z.; Yang, X. Capacity and mechanisms of ammonium and cadmium sorption on different wetland-plant derived biochars. *Sci. Total Environ.* **2016**, *539*, 566–575. [[CrossRef](#)] [[PubMed](#)]
- Ji, Z.-Y.; Yuan, J.-S.; Li, X.-G. Removal of ammonium from wastewater using calcium form clinoptilolite. *J. Hazard. Mater.* **2007**, *141*, 483–488. [[CrossRef](#)]
- Chen, S.-T.; Wickramasinghe, S.R.; Qian, X. High Performance Mixed-Matrix Electrospun Membranes for Ammonium Removal from Wastewaters. *Membranes* **2021**, *11*, 440. [[CrossRef](#)]
- Motlagh, A.R.A.; LaPara, T.M.; Semmens, M.J. Ammonium removal in advective-flow membrane-aerated biofilm reactors (AF-MABRs). *J. Membr. Sci.* **2008**, *319*, 76–81.
- Al-Ajalin, F.A.H.; Abdullah, S.R.S.; Idris, M.; Kurniawan, S.B.; Ramli, N.N.; Imron, M.F. Removal of ammonium, phosphate, and COD by bacteria isolated from *Lepironia articulata* and *Scirpus grossus* root system. *Int. J. Environ. Sci. Technol.* **2022**, *19*, 11893–11904. [[CrossRef](#)]
- IBI. *Standardized Product Definition and Product Testing Guidelines for Biochar That Is Used in Soil*; International Biochar Initiative: Canandaigua, NY, USA, 2012.
- Ahmad, M.; Rajapaksha, A.U.; Lim, J.E.; Zhang, M.; Bolan, N.; Mohan, D.; Vithanage, M.; Lee, S.S.; Ok, Y.S. Biochar as a sorbent for contaminant management in soil and water: A review. *Chemosphere* **2014**, *99*, 19–33. [[CrossRef](#)]
- Cui, X.; Wang, J.; Wang, X.; Khan, M.B.; Lu, M.; Khan, K.Y.; Song, Y.; He, Z.; Yang, X.; Yan, B.; et al. Biochar from constructed wetland biomass waste: A review of its potential and challenges. *Chemosphere* **2022**, *287*, 132259. [[CrossRef](#)]
- Cui, X.; Yang, X.; Sheng, K.; He, Z.; Chen, G. Transformation of Phosphorus in Wetland Biomass during Pyrolysis and Hydrothermal Treatment. *ACS Sustain. Chem. Eng.* **2019**, *7*, 16520–16528. [[CrossRef](#)]
- Gao, S.; DeLuca, T.H.; Cleveland, C.C. Biochar additions alter phosphorus and nitrogen availability in agricultural ecosystems: A meta-analysis. *Sci. Total Environ.* **2019**, *654*, 463–472. [[CrossRef](#)] [[PubMed](#)]
- Fan, R.; Chen, C.-L.; Lin, J.-Y.; Tzeng, J.-H.; Huang, C.-P.; Dong, C. Adsorption characteristics of ammonium ion onto hydrous biochars in dilute aqueous solutions. *Bioresour. Technol.* **2019**, *272*, 465–472. [[CrossRef](#)] [[PubMed](#)]
- Tang, Y.; Alam, S.; Konhauser, K.O.; Alessi, D.S.; Xu, S.; Tian, W.; Liu, Y. Influence of pyrolysis temperature on production of digested sludge biochar and its application for ammonium removal from municipal wastewater. *J. Clean. Prod.* **2019**, *209*, 927–936. [[CrossRef](#)]
- Zhao, Y.; Huang, L.; Chen, Y. Biochars derived from giant reed (*Arundo donax* L.) with different treatment: Characterization and ammonium adsorption potential. *Environ. Sci. Pollut. Res.* **2017**, *24*, 25889–25898. [[CrossRef](#)]
- Gai, X.; Wang, H.; Liu, J.; Zhai, L.; Liu, S.; Ren, T.; Liu, H. Effects of feedstock and pyrolysis temperature on biochar adsorption of ammonium and nitrate. *PLoS ONE* **2014**, *9*, e113888. [[CrossRef](#)]
- Bai, X.; Li, Z.; Zhang, Y.; Ni, J.; Wang, X.; Zhou, X. Recovery of Ammonium in Urine by Biochar Derived from Faecal Sludge and its Application as Soil Conditioner. *Waste Biomass Valorization* **2017**, *9*, 1619–1628. [[CrossRef](#)]
- Chandra, S.; Medha, I.; Bhattacharya, J. Potassium-iron rice straw biochar composite for sorption of nitrate, phosphate, and ammonium ions in soil for timely and controlled release. *Sci. Total Environ.* **2020**, *712*, 136337. [[CrossRef](#)]
- Liu, Z.; Xue, Y.; Gao, F.; Cheng, X.; Yang, K. Removal of ammonium from aqueous solutions using alkali-modified biochars. *Chem. Speciat. Bioavailab.* **2016**, *28*, 26–32. [[CrossRef](#)]
- Vu, T.M.; Trinh, V.T.; Doan, D.P.; Van, H.T.; Nguyen, T.V.; Vigneswaran, S.; Ngo, H.H. Removing ammonium from water using modified corncob-biochar. *Sci. Total Environ.* **2017**, *579*, 612–619. [[CrossRef](#)]
- Wang, S.; Ai, S.; Nziediegwu, C.; Kwak, J.-H.; Islam, S.; Li, Y.; Chang, S.X. Carboxyl and hydroxyl groups enhance ammonium adsorption capacity of iron (III) chloride and hydrochloric acid modified biochars. *Bioresour. Technol.* **2020**, *309*, 123390. [[CrossRef](#)] [[PubMed](#)]
- Amusat, S.O.; Kebede, T.G.; Dube, S.; Nindi, M.M. Ball-milling synthesis of biochar and biochar-based nanocomposites and prospects for removal of emerging contaminants: A review. *J. Water Process. Eng.* **2021**, *41*, 101993. [[CrossRef](#)]
- Zhang, Q.; Wang, J.; Lyu, H.; Zhao, Q.; Jiang, L.; Liu, L. Ball-milled biochar for galaxolide removal: Sorption performance and governing mechanisms. *Sci. Total Environ.* **2019**, *659*, 1537–1545. [[CrossRef](#)] [[PubMed](#)]
- Zheng, Y.; Wan, Y.; Chen, J.; Chen, H.; Gao, B. MgO modified biochar produced through ball milling: A dual-functional adsorbent for removal of different contaminants. *Chemosphere* **2020**, *243*, 125344. [[CrossRef](#)]
- Zhuang, Z.; Wang, L.; Tang, J. Efficient removal of volatile organic compound by ball-milled biochars from different preparing conditions. *J. Hazard. Mater.* **2021**, *406*, 124676. [[CrossRef](#)] [[PubMed](#)]

28. Feng, Q.; Chen, M.; Wu, P.; Zhang, X.; Wang, S.; Yu, Z.; Wang, B. Simultaneous reclaiming phosphate and ammonium from aqueous solutions by calcium alginate–biochar composite: Sorption performance and governing mechanisms. *Chem. Eng. J.* **2021**, *429*, 132166. [[CrossRef](#)]
29. Li, B.; Yang, L.; Wang, C.-Q.; Zhang, Q.-P.; Liu, Q.-C.; Li, Y.-D.; Xiao, R. Adsorption of Cd(II) from aqueous solutions by rape straw biochar derived from different modification processes. *Chemosphere* **2017**, *175*, 332–340. [[CrossRef](#)]
30. Bashir, S.; Zhu, J.; Fu, Q.; Hu, H. Comparing the adsorption mechanism of Cd by rice straw pristine and KOH-modified biochar. *Environ. Sci. Pollut. Res.* **2018**, *25*, 11875–11883. [[CrossRef](#)]
31. Chen, Z.; Xiao, X.; Chen, B.; Zhu, L. Quantification of chemical states, dissociation constants and contents of oxygen-containing groups on the surface of biochars produced at different temperatures. *Environ. Sci. Technol.* **2015**, *49*, 309–317. [[CrossRef](#)]
32. Zhu, K.; Fu, H.; Zhang, J.; Lv, X.; Tang, J.; Xu, X. Studies on removal of NH₄⁺-N from aqueous solution by using the activated carbons derived from rice husk. *Biomass Bioenergy* **2012**, *43*, 18–25. [[CrossRef](#)]
33. Hou, J.; Huang, L.; Yang, Z.; Zhao, Y.; Deng, C.; Chen, Y.; Li, X. Adsorption of ammonium on biochar prepared from giant reed. *Environ. Sci. Pollut. Res.* **2016**, *23*, 19107–19115. [[CrossRef](#)] [[PubMed](#)]
34. Yang, H.I.; Lou, K.; Rajapaksha, A.U.; Ok, Y.S.; Anyia, A.O.; Chang, S.X. Adsorption of ammonium in aqueous solutions by pine sawdust and wheat straw biochars. *Environ. Sci. Pollut. Res.* **2018**, *25*, 25638–25647. [[CrossRef](#)] [[PubMed](#)]
35. Rezaee, M.; Gitipour, S.; Sarrafzadeh, M.H. EVALUATION OF PHOSPHATE AND AMMONIUM ADSORPTION DESORPTION OF SLOW PYROLYZED WOOD BIOCHAR. *Environ. Eng. Manag. J.* **2021**, *20*, 217–227. [[CrossRef](#)]
36. Zhang, M.; Sun, R.; Song, G.; Wu, L.; Ye, H.; Xu, L.; Parikh, S.J.; Nguyen, T.; Khan, E.; Vithanage, M.; et al. Enhanced removal of ammonium from water using sulfonated reed waste biochar-A lab-scale investigation. *Environ. Pollut.* **2022**, *292*, 118412. [[CrossRef](#)]
37. Hu, X.; Zhang, X.; Ngo, H.H.; Guo, W.; Wen, H.; Li, C.; Zhang, Y.; Ma, C. Comparison study on the ammonium adsorption of the biochars derived from different kinds of fruit peel. *Sci. Total Environ.* **2020**, *707*, 135544. [[CrossRef](#)]
38. Wang, Z.; Guo, H.; Shen, F.; Yang, G.; Zhang, Y.; Zeng, Y.; Wang, L.; Xiao, H.; Deng, S. Biochar produced from oak sawdust by Lanthanum (La)-involved pyrolysis for adsorption of ammonium (NH₄⁺), nitrate (NO₃⁻), and phosphate (PO₄³⁻). *Chemosphere* **2015**, *119*, 646–653. [[CrossRef](#)]
39. Zheng, H.; Wang, Z.; Deng, X.; Zhao, J.; Luo, Y.; Novak, J.; Herbert, S.; Xing, B. Characteristics and nutrient values of biochars produced from giant reed at different temperatures. *Bioresour. Technol.* **2013**, *130*, 463–471. [[CrossRef](#)]

Disclaimer/Publisher's Note: The statements, opinions and data contained in all publications are solely those of the individual author(s) and contributor(s) and not of MDPI and/or the editor(s). MDPI and/or the editor(s) disclaim responsibility for any injury to people or property resulting from any ideas, methods, instructions or products referred to in the content.